THE CHARACTERIZATION AND COMPARISON OF BIOCHAR PRODUCED FROM A DECENTRALIZED REACTOR USING FORCED AIR AND NATURAL DRAFT PYROLYSIS

Leah Herbert, Ian Hosek, & Rishi Kripalani
Advisor: Dr. Linda Vanasupa

California Polytechnic State University, San Luis Obispo
Materials Engineering Department
4 June 2012

Approval Page

Project Title: THE CHARACTERIZATION AND COMPARISON OF BIOCHAR PRODUCED FROM A DECENTRALIZED REACTOR USING FORCED AIR AND NATURAL DRAFT PYROLYSIS

Author: Leah Herbert, Ian Hosek, & Rishi Kripalani

Date Submitted: 4 June 2012

CAL POLY STATE UNIVERSITY

Materials Engineering Department

Prof. Linda Vanasupa _____

Faculty Advisor Signature

Prof. Trevor Harding _____

Department Chair Signature

Acknowledgements

The Biochar team would like to recognize the Materials Engineering Department for the use of the equipment and labs, Professor Linda Vanasupa of the Materials Engineering Department, Craig Stubler of the Soil Science Department, and graduate student Cameron Danesh of the Chemistry Department. This project would not have been possible without their invaluable assistance.

Table of Contents

List of Figures

List of Tables

Abstract

The soil additive properties of biochar have proven both effective and globally beneficial, but depend heavily on feedstock used and process conditions. This study characterizes how forced and natural draft air flows affect the biochar's soil amendment potential. Biochars manufactured from two pine species of feedstock, in timber and pellet form, were compared against a designer biochar. The designer biochar held the lowest C:N ratio (57.43), followed by the natural draft pellets (199.5), forced air timber (282.5), forced air pellets (422.7), and natural draft timber (503.7). The designer char had the largest cation exchange capacity at 138.5 cmolc/kg; the decentralized biochars rated between 22.16 cmolc/kg and 62.33 cmolc/kg. X-ray diffraction failed to indicate the formation of turbostatic graphite, but confirmed the loss of organic content by the deflation of three broad cellulose peaks between 14.88-22.78°; expected mineralogical restructuring was confirmed in the designer biochar. Fourier-transform infrared spectroscopy confirmed the reduction in aliphatic functional groups (2820-2980 cm^{-1}) and but failed to prove the formation of aromatic carbon-carbon double bonds (1580-1610 cm^{-1}) after pyrolysis. Using scanning electron microscopy, draft conditions were concluded to have little or no effect on pore morphology. In order to help gauge the agricultural benefits of these biochars, an additional soil study is recommended to observe how soil interactions with the biochar affect the CEC and the C/N ratio over time.

Key Words

Biochar, characterization, cation exchange capacity, FTIR, XRD, carbon nitrogen ratio, decentralized reactor, Materials Engineering

1 Introduction

1.1 Problem Statement

This study characterizes and compares the physical and chemical properties of biochar produced using a decentralized reaction. Characterization of the biochar encompasses surface morphology, compositional analysis, and soil additive potential. The benefits of biochar arise from: creation of the byproducts (bio oil and syngas), reduction in greenhouse gases associated with agricultural development, nutrient and moisture retention, reduction in fertilizer use, increased integration of microbial population with soil, and stabilization of pH in favorable ranges.

1.2 History of Biochar

Using charcoal as a soil amendment first began over 2,500 years ago in the Amazon Basin, South America [1]. It is unclear whether the Amazonian people intentionally created *terra preta* ("black earth"), or if it was simply the byproduct of their slash and burn practice. These soils continue to exhibit enhanced fertility via higher carbon and nutrient content even thousands of years after their implementation. Most notably, crops cultivated in the black soil are reported to grow three times faster than those in surrounding land. Furthermore, the largest impact demonstrated by biochar addition occurs in highly acidic or nutrient depleted soils [2].

The thermal degradation of biomass is essential to producing the atmospheric and soil benefits; not all graphitic carbon presents the same properties of biochar. Tire materials, plastics, and activated carbon have all been tested, but often times the impacts are detrimental to plant and soil life [1].

1.3 Broader Impacts

The thermal degradation of biomass produces three products: char, bio-oil, and syngas. The bio-oil and syngas are able to be captured and used for energy purposes as heat or biofuel in transportation or electricity production. The remaining solid, biochar, has a multitude of applications, including agricultural (Figure 1).

Biochar promotes plant growth with its high degree of porosity, capitalizing on capillary forces to further increase water retention; the porous structure includes many active negative sites, thus increasing nutrient adsorption capacity and retention. Due to greater nutrient retention, biochar limits the necessity for fertilizer and also decreases soil erosion. Biochar also stabilizes the pH in the favorable range of 5-6.4 pH.

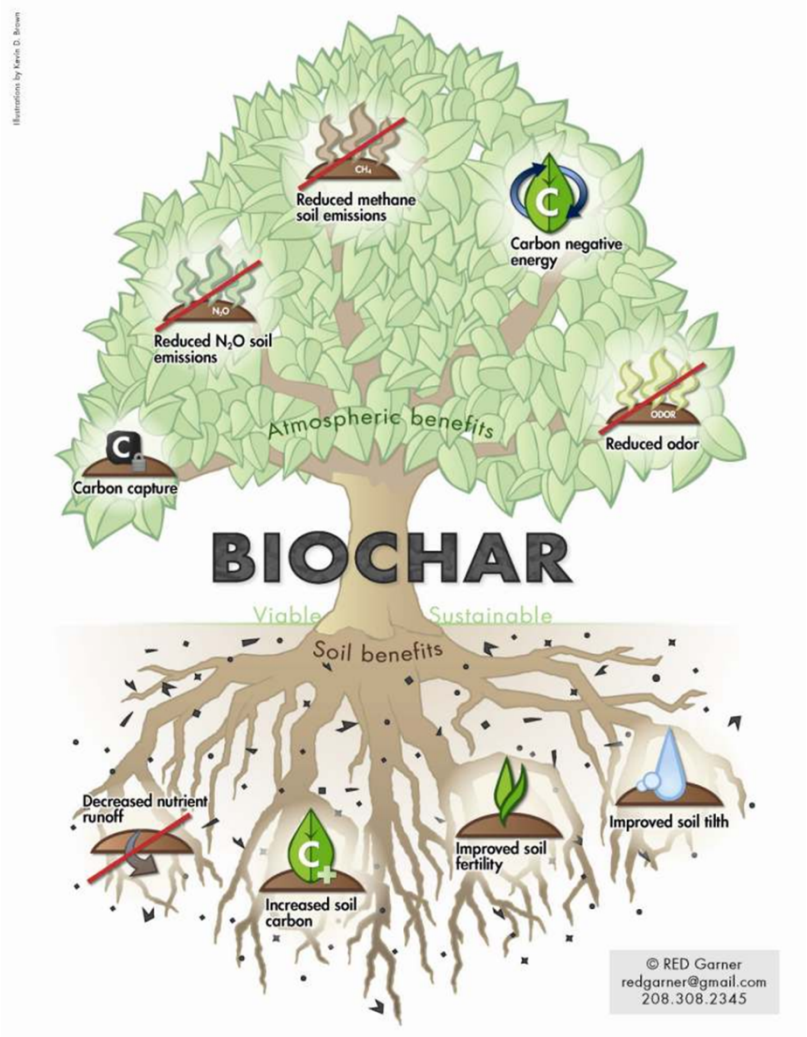

Figure 1: Biochar has both atmospheric and soil benefits [3].

Agricultural emissions of greenhouse gases (GHG) are causally linked to 13.5% of climate change. Research has demonstrated that soil amended with biochar reduces greenhouse gas (GHG) production, specifically CO_2, N_2O, and CH_4. Biochar has mitigated GHGs anecdotally via reduction of N_2O emissions by 50% in soybean plots and almost completely suppression of CH_4 release in the Eastern Colombian Plains. Biochar is also carbon negative-- it sequesters more CO_2 than produced and provides a reduction in anthropogenic CO_2 emissions by up to 12% [3] (Figure 2).

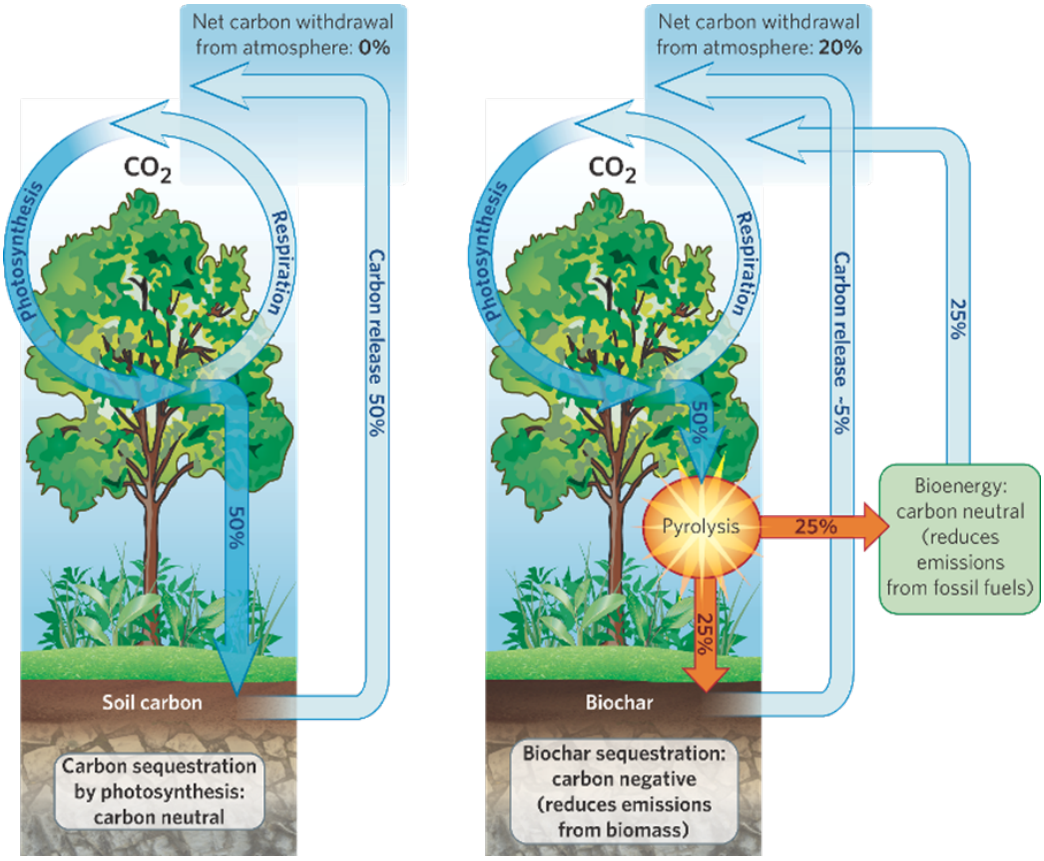

Figure 2: The thermal degradation of biomass into biochar is inherently a carbon negative process .

The ease of manufacturability of biochar allows close control of production method and scale. With this capability, many feedstocks are viable and biochar properties can be specifically tailored to a region or application. This allows it to be independent of geographical location or climate and demonstrates the versatility of the pyrolysis process. For specific properties, a highly controlled laboratory process may be implemented. Conversely, a less stringent process can be produced from a decentralized reactor. By having a decentralized process, low profit agricultural operations are able to treat their topsoil with minimal purchasing costs.

1.4 Properties of Biochar

Biochar is a type of charcoal and is formed through the decomposition of biomass through pyrolysis with byproducts of bio-oil and syngas. Biochar only differs from charcoal in its intent: biochar is produced specifically for soil application, whereas charcoal has a multitude of applications. Biochar and its byproducts can be produced from a wide variety of feedstocks such as organic farm waste, waste treatment plant slurry, and woods with high cellulose/lignin content. After pyrolysis, the solid byproduct is a porous network of carbonates and/or aromatic carbon.

Biochar is a natural host for raw soil materials such as fertilizers, microbes, and plants. It is not directly consumed by plants but instead acts as a catalyst for beneficial soil reactions [4]. Without thermal modification, all forms of biomass are biodegradable. The thermal transformation of pyrolysis releases volatile gases as the carbon atoms rearrange into a new solid structure; this reaction occur over a temperature range of 200-500℃. The pyrolytic gases are released into the atmosphere, unless otherwise caught [1].

Above 300℃, carbonization occurs and the chemical bonds undergo dehydration and aliphatic bonds are converted into aromatic bonds; these aromatic bonds grow together to form local grapheme complexes [1]. The covalent bonds between the structures protect the bonds from living systems breaking down the graphitic structure. Furthermore, the pore walls of the biochar act as active sites for cation exchange without consuming any of the vital nutrients (Figure 3). This allows all pertinent minerals to be accessed easily by plant roots and microbes.

Pyrolysis throttles certain chemical reactions; specifically, the major components of biomass, hemicellulose, lignin and cellulose, transform at different temperatures. Naturally, various types of pyrolysis occur depending on burn temperature (Table I).

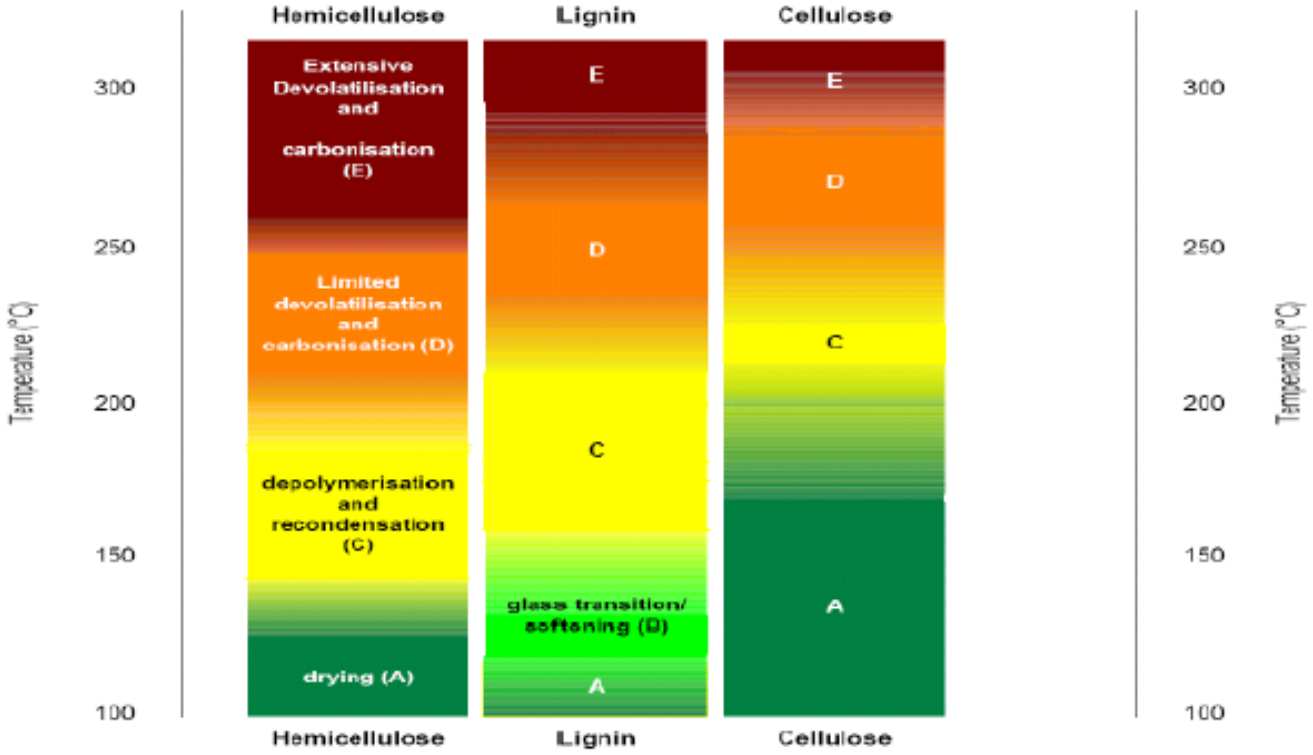

Figure 3: Thermal modification temperature range for hemicellulose, lignin, and cellulose [1].

Table I: Bio-oil, syngas, and biochar yield as dependent on pyrolysis temperature [2]

Mode	Condition	Bio-oil	Biochar	Syngas
Fast pyrolysis	Moderate temperature (~500℃), Short vapor residence time (<2s)	75% (25% water)	12%	13%
Intermediate pyrolysis	Low-moderate temperature, moderate hot vapor residence time	50% (50% water)	25%	25%
Slow pyrolysis	Low-moderate temperature, long residence time	30% (70% water)	35%	35%
Gasification	High temperature (>800℃), long vapor residence time	5% tar (55% water)	10%	85%

1.5 Soil Amendment

Biochar's application can increase plant growth rates via to its ability to increase nutrient and water retention of soil, which decreases strain on the root system to provide sustenance. It has also been proven to reduce greenhouse gas emissions (GHG), aid in pH control, sequester carbon dioxide (CO_2), aid in toxicity mitigation, and is scalable for the home gardener to the industrial farmer.

1.5.1 Ease of Application

Biochar has the ability for large impact in the agricultural world due to its ease of application. Application techniques can be manipulated based on farming system, and available labor and machinery [2]. Methods of application include: mixing with fertilizer and seed, top-dressed (on soil surface), uniform soil mixing, no till systems, deep banding with or without plow (below surface 0.1-0.2 m), mixture of compost and char, and top layer at planted edges (to catch run-off) [2].

1.5.2 Nutrient Retention

Biochar addition to soil has shown a greater increase of exchangeable Ca, Mg, K, Na, and P in the soil (Figure 4) [5]. This creates an environment with an elevated cation exchange capacity (CEC). The CEC measures how well cations are bound to soil or biochar and are then prevented from leaching into the ground [5]. The negatively charged reactive surface of biochar allows for cations to be electro-statically bounded (adsorbed) and available for exchange with the plant roots.

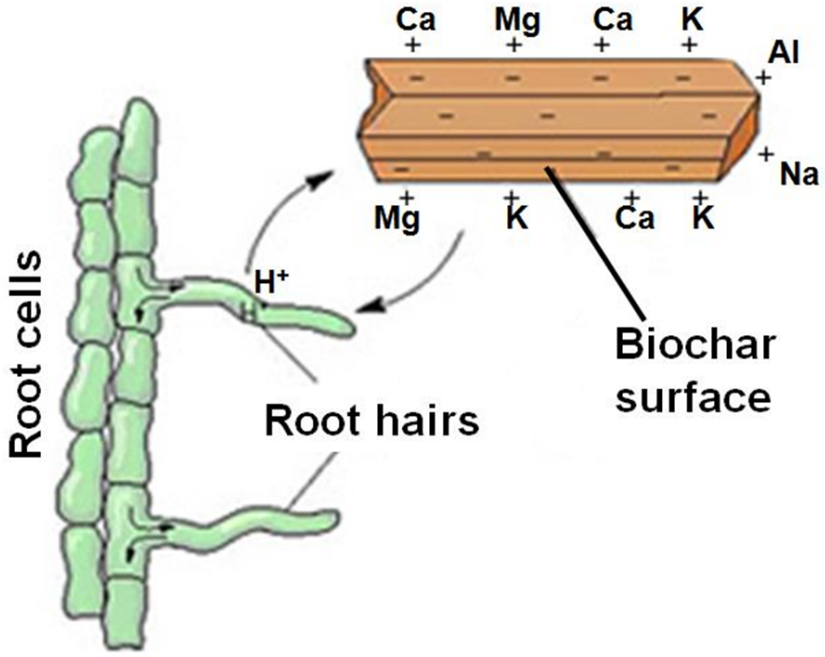

Figure 4: Through the addition of biochar, the cations are held closer to the roots preventing leaching into soil and ground water

The aging or weather of biochar and its effect on soil properties has been of increasing interest [6]. The aging of biochar initiates after its creation, even prior to soil integration as a function of the storage environment, most notable the atmospheric temperature and moisture. Furthermore, the moisture content has a large impact on the role of biochar interaction with soil, specifically the dissolution, hydrolysis, carbonation, decarbonation, reduction/oxidation, and soil organism interaction. Some literature states that as it ages the CEC will increase, other literatures believe it will disintegrated through tillage and wreathing of the soil [5].

1.5.3 pH control

When biochar is first added to the soil, the reactive surface allows cations to accumulate and increase the pH [7]. The pH properties of biochar change after the sample has adjusted to atmospheric carbon dioxide; during this transformation the alkaline hydroxides react to form carbonates and lowers the pH. [1]. As the biochar ages, the concentration of basic sites decreases through oxidative interactions with microbes [6]. Functional groups that are often formed during this interaction include carboxylic, lactonic, phenolic, carbonyl, o-quinone-like structures, and ether-type oxygen. The first three functional groups most affect cation exchange capacity for biochar particles [6].

1.5.4 Moisture retention and aeration

The high surface area of biochar can lead to increased water retention [5]. In sandy soil, when 45% by volume of biochar was integrated with the soil, the available moisture increased by 18% due to the porosity of biochar (increased surface area to volume ratio). Since the moisture retention is highly dependent on the size of the pores (with micro-pores being optimal for capillary forces), the biochar feedstock and soil texture are highly influential [5].

2 Biochar Reactors

The technology involved in pyrolysis reactors varies greatly between batch (decentralized), continuous (centralized), and novel processes (centralized) [2]. For the purposes of this paper, decentralized reacts can be built with minimal technology require minimal effort to produce biochar, and are inefficient in operation leading to low yields. These processes do not allow for the capture of syngas and bio-oil. Continues and novel processes, *centralized reactors*, result in higher biochar yields. Feedstock flexibility increases and may allow for byproduct capture, but these higher technology processes are also more expensive than batch processing (Figure 5)

Figure 5: Continues reactors or centralized reactors are more complex systems but also produce higher yields and allows for the capture of syngas and bio-oil . (a) BEST Energies paddle drum dlow pyrolysis reactor. (b) Pro-Natura'sPyro-7 continues flow screw type reactor is able to produce co-generation of char and energy, but has no usable byproducts.

Decentralized reactors (specifically batch processes) have the lowest yield of char, ranging from 10-30%, and are traditionally constructed into the earth. The reactor type rages from earth pits and mounds, brick, concrete and metal kilns, and retorts (Figure 6).

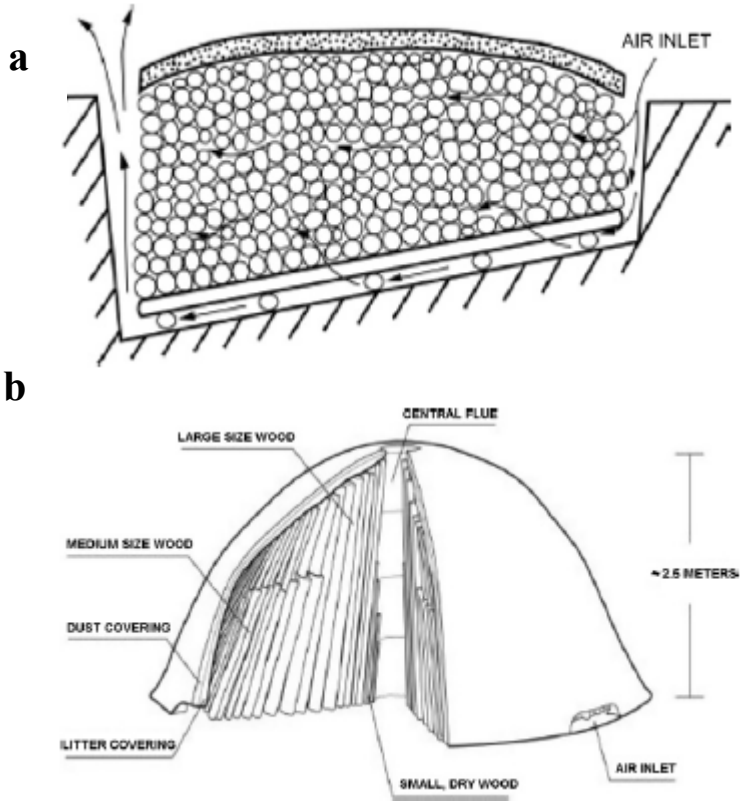

Figure 6: (a) A pit kiln uses natural convection supplied by the construction into the earth. (b) A mound kiln's pyrolysis process produces a considerable amount of heat and maybe also used as a heating source [2]

The Top-Lift UpDraft (TLUD) is a small scale, decentralized pyrolytic gasifier [1]. This reactor features flaming pyrolysis, char is produced simultaneously as pyrolytic wood gas is released from the biomass. The heat co-produced by this reactor has been of interest in ongoing research. In this reactor, the biomass is stationary with the exception of shrinkage due to combustion. A pyrolysis front moves downward through the reactor after the top of the biomass is ignited by an outside source. The main combustion air is pulled upward from beneath the biomass by holes punched into the reactor. This mode of combustion, "flaming pyrolysis", is different than the "glowing pyrolysis" of the previous decentralized reactors; in this reaction, the biomass is converted into char and combustible volatiles are released through the heating duct:

The tiny "flames" within the descending pyrolysis front are due to the combustion of a portion of the created pyrolysis gases, thereby generating the heat needed for propagating the pyrolysis front downward. Since the rate of heat generation is determined by the amount of available oxygen, the progression of the pyrolysis front is controllable by regulating the primary airflow. In a typical TLUD, the pyrolysis front moves downward 5 to 20 mm per minute, depending on the nature of the fuel and the amount of available primary air (Figure 7).

Above the pyrolysis front, the created char accumulates and the oxygen-depleted air (mainly nitrogen, carbon dioxide, carbon monoxide and water vapor) sweeps the created pyrolytic gases to the secondary combustion zone. There, additional air is provided and the pyrolytic gases are burnt in a separate and very clean flame. These pyrolytic gases are tarry and long-chain hydrocarbons that, if not burned, would form a thick smoke.

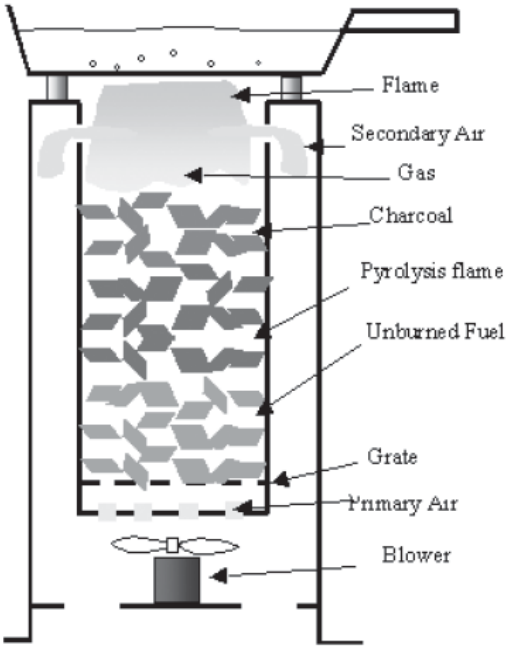

Figure 7: TLUD with forced air attachment allows for a clean burn [8].

.

2.1 Measurement of Biochar Quality

2.1.1 Carbon / Nitrogen Ratio

The carbon-nitrogen ratio (C/N) demonstrates the ability for an organic substrate to release inorganic nitrogen when mixed with soil [5]. The carbon content of biochar ranges from 1-80% and is dependent on the feedstock (both type and preprocessing conditions) and the thermal degradation due to pyrolysis [9]. Biochar's C/N varies between 7 and 500 [5]. High C/N ratios may lead to nitrogen immobilization after

biochar soil application [7]. In practice, biochar is often pretreated with a nutrient rich source such as compost to impregnate the biochar with nitrogen and excess nutrients.

3 Methods and Materials

3.1 Reactor Fabrication

The reactor design was adapted from the 1G Toucan TLUD [10]. The TLUD reactor was constructed with the following materials: 1 gallon paint can, #10 can, and a 3 foot long heating duct. The primary air flow entry points were created by having a series of symmetric holes punched into the base gallon paint can using a punch (Figure 8)

Figure 8: The main reactor chamber bottom. The pattern directs the primary airflow into the system.

A crown was created from the #10 can by cutting down to 2.5 inches using tin snips followed by a patterning effect with a permanent marker. The cylinder walls had 8 equally spaced equilateral triangles and holes marked around the perimeter and then the excess material was removed with tin snips. A 3 inch diameter circle was removed from the base of the cylinder, allowing a pathway for secondary airflow. Modifications of the #10 can were finished by folding the tabs of excess material located between the triangular holes back towards the center (Figure 9). This allowed for the can to stabilize itself and sit firmly on top of the paint can.

Figure 9: The crown of the biochar reactor. The 3 inch hole and eight triangles have been cut. The tabs between the triangles have been folded inwards.

The forced air attachment was tailored from a design created by Hugh McLaughlin [11]. The TLUD forced air attachment was produced from a 1 gallon paint can, a 28 ounce tin can, a hose clamp, an 80 millimeter computer fan, four lengths of small diameter rope, and electrical tape. First, the paint can had a large hole cut into the side of it to fit the diameter of the 28 ounce tin can. The pattern for this cut was made by placing the tin can on the wall of the 1 gallon paint can and tracing the diameter. Next, lines radiating from the center of the new circle were drawn and then cut. This created tabs that would allow the tin can to be latched to the paint can. The 28 ounce tin can was then inserted into the newly cut hole and the tabs were folded down and secured in place with the hose clamp. Several gaps between the tin can and 1 gallon paint can were observable; electrical tape was wrapped around the binding site to form a seal. The computer fan was then strapped to the 28 ounce can by punching four evenly spaced holes near the end furthest away from hose clamp. The four pieces of rope were then threaded through the new holes and the fan assembly. Each rope was tightened and fastened so the center point of the fan was aligned with the center point of the 28 ounce can. Again, electrical tape was used to create a seal between the can and the 80 millimeter fan (Figure 10).

Figure 10: The forced air attachment. Electrical tape was used to create a good seal between the two connection points.

3.2 Feedstocks and Preparation

Two different pine feedstocks were used in this study to examine how preprocessing affects the biochar. Eagle Valley wood fuel pellets used for wood stoves was the first feedstock (Figure 11). These pellets are created from sawmill wood waste that is gathered then compacted in the radial direction.

Figure 11: Eagle Valley wood fuel pellets. They are composed of compacted pine from sawmill waste.

The pellets are 6 millimeters in diameter and generate less than 0.5% ash when allowed to go through the secondary combustion phase [12]. The second feedstock used was ponderosa pine timber milled by Sierra Pacific Industries [13]. The lumber was 1" x 4" x 24" (Figure 12**)**. In order for the timber to fit into the main biochar reactor chamber it was hand chopped into pieces less than 10 cubic inches.

Figure 12: Ponderosa pine timber from Sierra Pacific Industries. The pieces were chopped parallel to the length of the grain.

3.3 Biochar Production

Two different methods were used for biochar production. The first process was natural draft airflow while the second was forced draft airflow. The natural draft production technique used a natural convection current, created by rising heat that draws air from below through the feedstock to fuel the combustion reaction. In the forced draft production technique, the combustion reaction was fueled with air from an 80 millimeter computer fan that produced airflow of 24 cubic feet per minute. There was sufficient forced convection to ignore mixed heat transfer modes.

The preliminary setup for natural draft and forced draft production were the same except the addition of the forced air attachment. Both procedures began by placing the feedstock in the reactor chamber; for pellet biochar the reactor was filled until the pellets were approximately 2 centimeters below the rim of the paint can. The timber biochar had the entire plank of chopped lumber inserted into the chamber in a fashion that allowed for a more unhindered airflow than the pellets. The longer pieces were oriented along the vertical axis of the paint can while the shorter pieces were randomly oriented. After this initial step the natural draft and forced draft procedures differed in several ways.

For natural draft conditions, the reactor was placed on four equally spaced screws that provided an air gap between the ground and the base of the paint can. Once this was completed, a small amount of lighter fuel was added to the topmost portion of the feedstock (~ 4 milliliters). The crown was then placed on the top of the reactor and the feedstock was ignited using a match. Finally the heating duct was centered on top of the crown to increase draft rate and a rock was placed on top to stabilize the system (Figure 13)

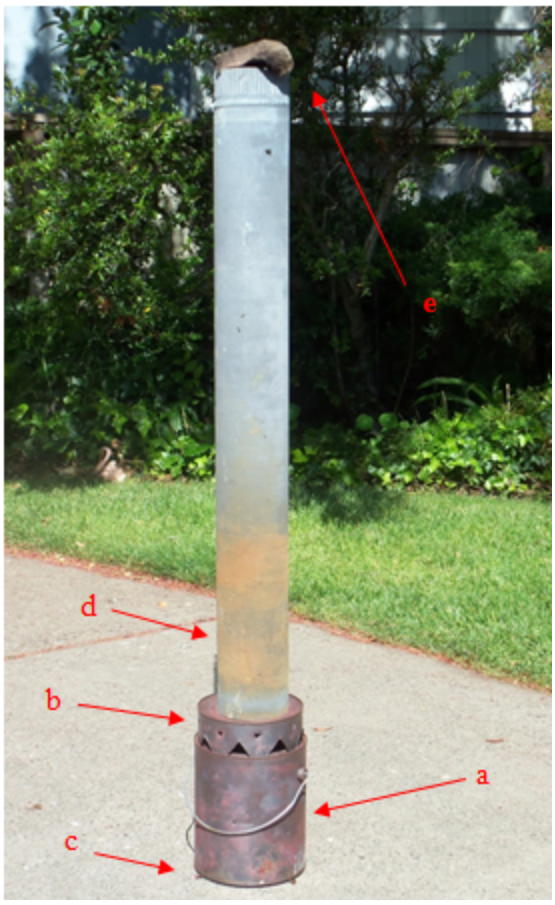

Figure 13: The natural draft biochar production setup. (a) Reactor chamber (b) Crown (c) Screws (d) Heating Duct (e) Stabilization rock

The pyrolysis process was then monitored through careful observation. The combustion reaction was quenched once primary combustion of the feedstock had taken place and secondary combustion of the char was under way. Several indicators were used to determine when secondary combustion began: a large amount of thick smoke started to be produced from the top of the heating duct, the combustion flame turned from orange-yellow to blue, or the flames that indicated primary combustion were extinguished. The system was quenched by first removing the rock, heating duct, and crown. Proper heat protection equipment was used to help avoid unnecessary burns. Next the reactor was lifted, using the handle, and placed firmly on solid ground that was able to withstand high temperatures. The lid of the paint can was then pounded using a rubber mallet onto the top to create a seal. This prevented any further oxygen from contaminating the system. The reactor and biochar were then allowed to cool to room temperature. After cooling, the lid was removed from the paint can and the biochar was transferred into a Ziploc bag for storage and further analysis.

The forced draft followed a similar procedure but differed in several distinct areas. After the feedstock was inserted into the reactor the system was placed on top of the forced air attachment. The bottom of the reactor chamber and rim of the forced air assembly were concentrically aligned to decrease leakage and maximize airflow. Next the protruding can and fan were stabilized using two small pieces of wood. After stabilization, the fan was powered with a variable voltage source which was set to 12 volts. The remaining steps followed the natural draft procedure for igniting the feedstock (Figure 14)

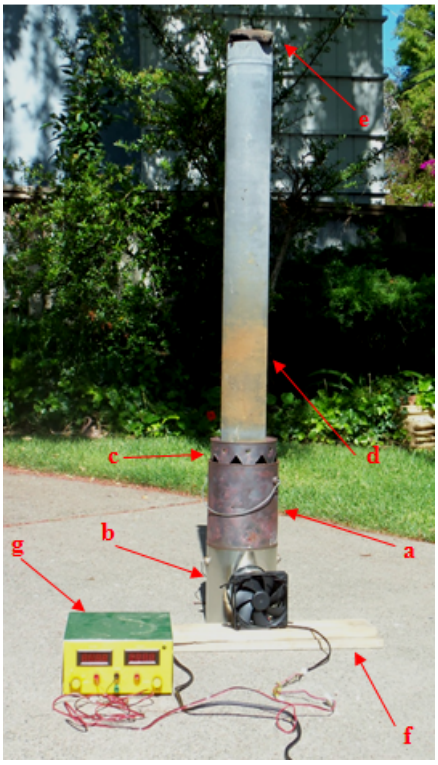

Figure 14: The forced air biochar production setup. (a) Reactor chamber (b) Forced air attachment (c) Crown (d) Heating duct (e) Stabilization rock (f) Stabilization boards (g) Variable voltage source

Each feedstock and pyrolysis process created different reaction temperatures and times. Pyrolysis times were measured from when the feedstock was lit until when the reactor was quenched using a standard stop watch. In order to measure the maximum pyrolysis temperature of the system a k-type thermocouple was inserted approximately half way down into the side of the reactor chamber amidst the feedstock. Table II shows how the pyrolysis time and max pyrolysis temperature varied under the production conditions.

Table II: Reaction Times and Maximum Temperatures for Biochar Production

Pyrolysis Conditions	Reaction Time	Maximum Pyrolysis Temperature (°C)
Natural Draft Pellet	1 hr 28 min 45 sec	657
Forced Draft Pellet	48 min 53 sec	939
Natural Draft Timber	19 min 12 sec	817
Forced Draft Timber	15 min 42 sec	894

3.4 Cation Exchange Capacity

3.4.1 CEC From Summation of Cations

The CEC of the biochars were obtained using two different methods developed at Cal Poly's soil science laboratory**Invalid source specified.**. The first method measured the summation of cations adsorbed to the biochar surface by replacing them with ammonium ions. Four grams of each powder sample was placed into 50 milliliter centrifuge tubes and 20 milliliters of 1 *M* NH_4OAc (ammonium acetate) was added. Then the centrifuge tube was shaken on a reciprocating shaker for 30 minutes. After all of the powder had been suspended in solution, the contents of the tube was poured through a Whatman No. 1 filter paper into a 100 milliliter volumetric flask. The tube was then further rinsed and filtered with ammonium acetate to remove biochar that had stuck to the sides of the container (Figure 15).

Figure 15: The filtering step for determining the CEC using the summation of cations.

The volume of the solution was next brought up to 100 milliliters using more NH_4OAc. The solution obtained at this point in the procedure was known as the original extract. From the original extract dilutions of 20x, 40x, and 80x were created. After the dilutions had been separated into various volumetric flasks, atomic absorption spectroscopy (AAS) was used to determine the concentrations of the various cations. Because Ca^{2+}, Mg^{2+}, K^{+}, and Na^{+} are the main cations contained within biomass, these were measured to best describe the CEC. When measuring Ca^{2+} and Mg^{2+} concentrations, all of the original extracts were used for the corresponding biochar except for the designer extract; a dilution was required to mitigate AAS saturation. When measuring K^{+} concentrations, all extracts required dilution to prevent detector saturation. 20x dilutions for natural draft pellet and natural draft timber extracts were necessary, yet forced air pellet and forced air timber extracts required 40x dilutions. In order to obtain an accurate K^{+} concentration for the designer biochar, a dilution of 80x had to be used. Na^{+} concentrations were found from the original extracts of natural draft and forced draft pellet biochar and using 20x dilutions for the natural draft timber, forced draft timber, and designer extracts.

From these different cation concentrations individual CECs were determined by:

$$CEC\ (individual\ cation) = \frac{mg}{L} * Dilution\ Multiplier * \frac{100\ mL}{4\ g\ biochar} * \frac{1\ L}{1000\ mL} * \frac{1000\ g}{1\ kg} * \frac{mmol}{At.wt.mg} * \frac{cmol}{10\ mmol} * Cation\ Charge$$

Equation 1

When each of the four cation concentrations for a specific biochar had been found then they were summed and the final value was the experimental CEC.

3.4.2 CEC from Adsorbed $NH4^+$

The second method used to determine CEC measured how much NH_4^+ was adsorbed by the biochar during the cation extraction process in the previous method. After the solution was poured through the filter paper, the filter papers were removed and placed back into their corresponding centrifuge tubes. Next 25 milliliters of isopropanol was added to the tube and then the solution was shaken for 10 minutes on a reciprocating shaker. This was done to remove any remaining ammonium ions not bonded to the active sites on the biochar surface. Next, the tube was placed in a centrifuge and ran at 2000 rpm for 5 minutes. After the desired time had elapsed the tube was removed and the solution was decanted. 25 milliliters of isopropanol was again added and the tube was vortex mixed and shaken on the shaker for 5 minutes. The same centrifuge procedure was performed after the shaking and it was decanted a second time. Afterwards, 50 milliliters of KCl (2 M) was added to the biochar pellet and vortexed then mixed in a 250 milliliter wide-mouth Erlenmeyer flask. The solution was filtered through another No. 1 filter paper into a 100 milliliter volumetric flask. Next a pipette was used to transfer 20 milliliters of extract into a 250 milliliter beaker. One milliliter 1 M NaOH was added to the solution and then the concentration of NH_3 was read after one minute using an ammonia probe. The NaOH reacts with ammonium to create a mixture of water and ammonia; once the concentration of NH_3 had been measured, the total CEC for the biochar was calculated using Equation 1.

3.5 Scanning Electron Microscope

Surface morphology was examined in high vacuum (10^{-6} torr) using a thermionic scanning electron microscope (FEI Quanta 200) to establish macro-pore shape and relative frequency. All samples were Au-sputtered to reduce charge effects.

3.6 X-Ray Diffraction

X-ray diffraction was performed on the feedstocks and biochars using a Siemens D5000 Diffractometer. Three grams of each char were granulated for powder diffraction using Cu $K_{\alpha 1}$ radiation (40 kV, 40 mA) from 5° to 65° (2θ) with 0.1 step size and 2 second measurement interval. Feedstock samples were sectioned and mounted planar to the source/detector to minimize scattering.

3.7 FTIR

Fourier-Transform Infrared Spectroscopy was conducted in atmosphere using a Nicolet Nexus 470. An absorbance spectrum (600-4000 cm^{-1}) was collected with 4 cm^{-1} resolution for each 5 mg granulated sample of feedstock/biochar and normalized against atmospheric background.

3.8 Carbon / Nitrogen Ratio

An Elementar Vario Max CNS was used to determine the total C and N concentrations through dry combustion. The C/N ratio was further calculated. The combustion, post-combustion, and reduction temperatures were respectively chosen as 900°C, 900°C, and 830°C. The machine was calibrated by two blanks (empty crucibles), 2 runin (glutamic acid), and 3 glutamic acid samples. The five biochar samples were then tested followed by known plant samples. These samples were tomato and soil and were run to ensure accuracy. The biochar was ran under plant specifications. Each sample had a specific method to ensure proper readings (Table III).

Table III: Elementar Vario Max CNS Testing Method

	Blank	Plant	Soil	Glutamic Acid
Weight ca. (mg)	100 (machine configuration)	300	300	300
Auto. Zero Delay (sec.)	120	60	60	120
Peak Anticipated N (sec.)	50120	270	270	240
O_2 Dosing Time (sec.)	5050	120	120	120
O_2 Dosing (mL/min)	1550	125		125
O_2 Threshold (%%)	015	15	15	15
Peak Max (%)	0	0	0	0
Kjeldahl Factor	1.00	1.00	1.00	1.00

Standard samples were used for calibration. First, a medium content soil (standard OAS, B2178, BN/155563, certificate 115255) and contained 0.27% nitrogen and 3.19% carbon. Second, known tomato leaves (adhering to NIST Standard Material 1573A) had nitrogen levels of 3.03%, 0.96% sulfur, and an approximate carbon content of 36.2%. Third, glutamic acid (produced by Alfa Aesar, Stock #A15031/L07684, Lot #J19W024, CAS #56-86-0) with above 99% purity had a known carbon content of 40.78% and a nitrogen content of 9.52%.

4 Results

4.1 Cation Exchange Capacity

Due to the nature of each method for determining the CEC of biochar, CECs found using the Summation of Cations method will not be reported or discussed. They were used as relative comparisons and portrayed the same trends as the CECs found from ammonium adsorption. NH_4^+ adsorption is a more accurate technique for the total CEC and was examined in greater detail.

The corrected CEC values (in centimoles charge per kilogram of mass) for each biochar feedstock and production method give insight into what parameters influence the biochar's ability to exchange cations with the surrounding soil and biological organisms (Figure 16).

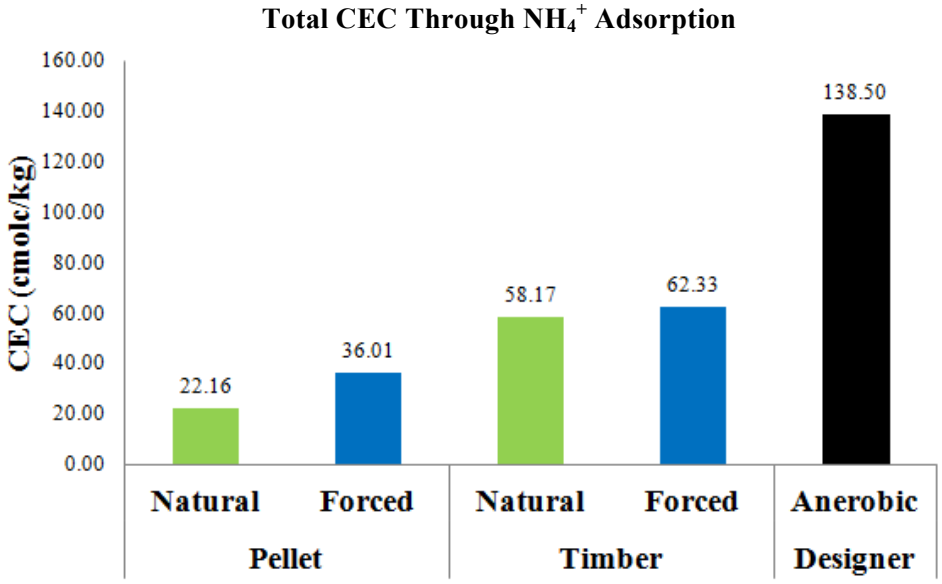

Figure 16: CEC values for the various biochars found through ammonium adsorption and extraction using KCl.

The designer biochar has the highest cation exchange capacity out of all of the chars at 138.50 cmolc/kg. The timber biochars have similar CECs around 60 cmolc/kg while the pellet biochars produced using different processes have statistically different values. The natural draft pellet biochar had a lower CEC of 22.16 cmolc/kg while the forced draft pellet biochar had a higher CEC of 36.01 cmolc/kg. Statistical analysis was unable to be performed on the collected data due to the small sample size. The methodology for obtain CEC values was time consuming and wasteful of the reagents used and therefore was not repeated.

4.2 Scanning Electron Microscope

Draft conditions manifested no noticeable differences in pore morphology, but significant structural differences were found between feedstock preprocessing conditions (Figure 17). Timber biochars show intermittent elliptical pores 50-200 μm in diameter spaced between longitudinal sheets of pyrolysized precursor (a). Transverse cavities between these sheets form channels with diameters less than 1 μm, evident by the partial fracture of the top-face sheet layer (b). Pellet biochars exhibited a macroscopic peeling or flaking of compression layers (c); resulting pores appear to be gaps in the random overlap of fibrous matter (d). Cavities between flaked layers produce pores greater than 100 μm in diameter (e).

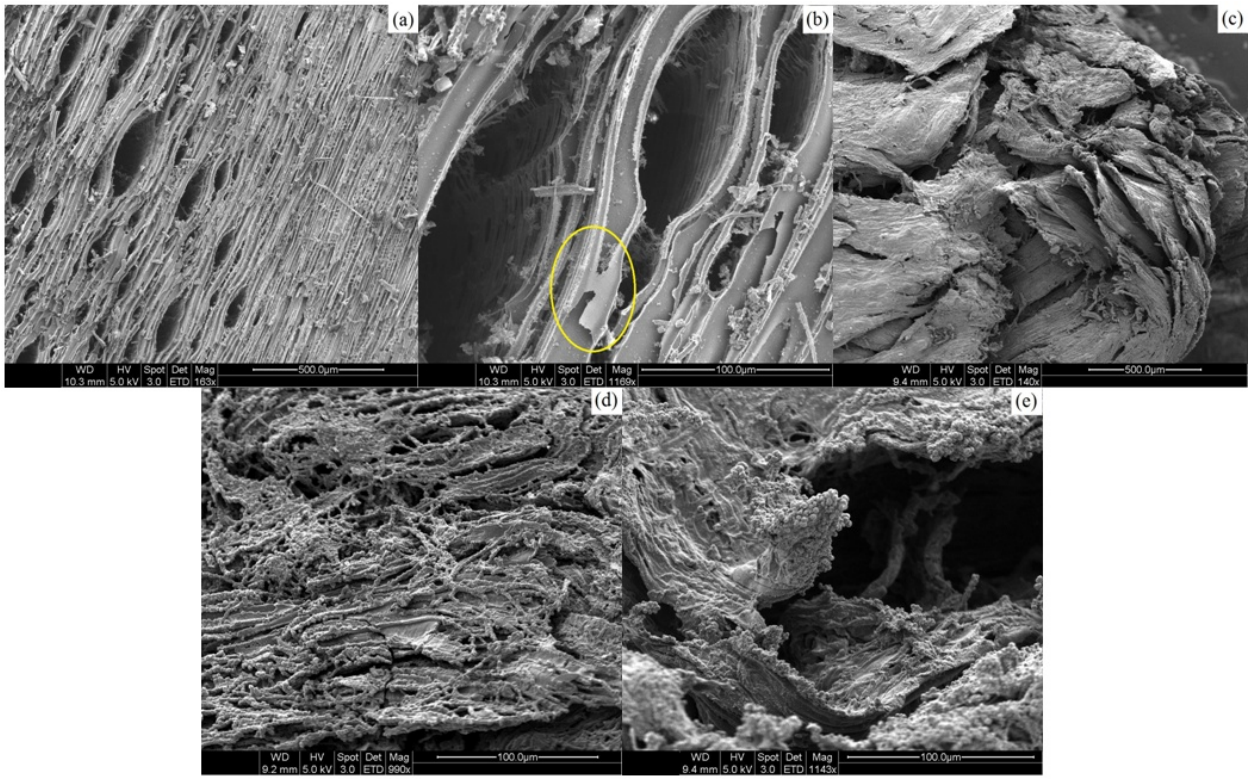

Figure 17: SEM micrographs of (a and b) natural draft timber, (c and e) natural draft pellet, and (d) forced air pellet biochars.

4.3 X-Ray Diffraction

Complex organic molecules are inherently amorphous, but XRD is a viable tool for identifying the matrix of linear D-glucose chains in cellulose I feedstock. Cellulose I is expressed by three broad characteristic peaks centered on 14.8°, 16.2° and 22.7° (2θ) [14]. No evidence of graphite appeared on the pine biochars produced, regardless of preprocessing or draft conditions (Figure 18 a & b).

Sharp peaks in the diffractogram of designer biochar indicate whewellite [$Ca(C_2O_4)\cdot H_2O$] and calcite [$CaCO_3$] consistent with its pyrolysis temperature Figure 17c. Pyrolysis temperatures above 700°C decompose calcium oxalate [$Ca(C_2O_4)$] to volatiles and carbon dioxide [15]. This decomposition is observed in the pine biochars produced within this experiment.

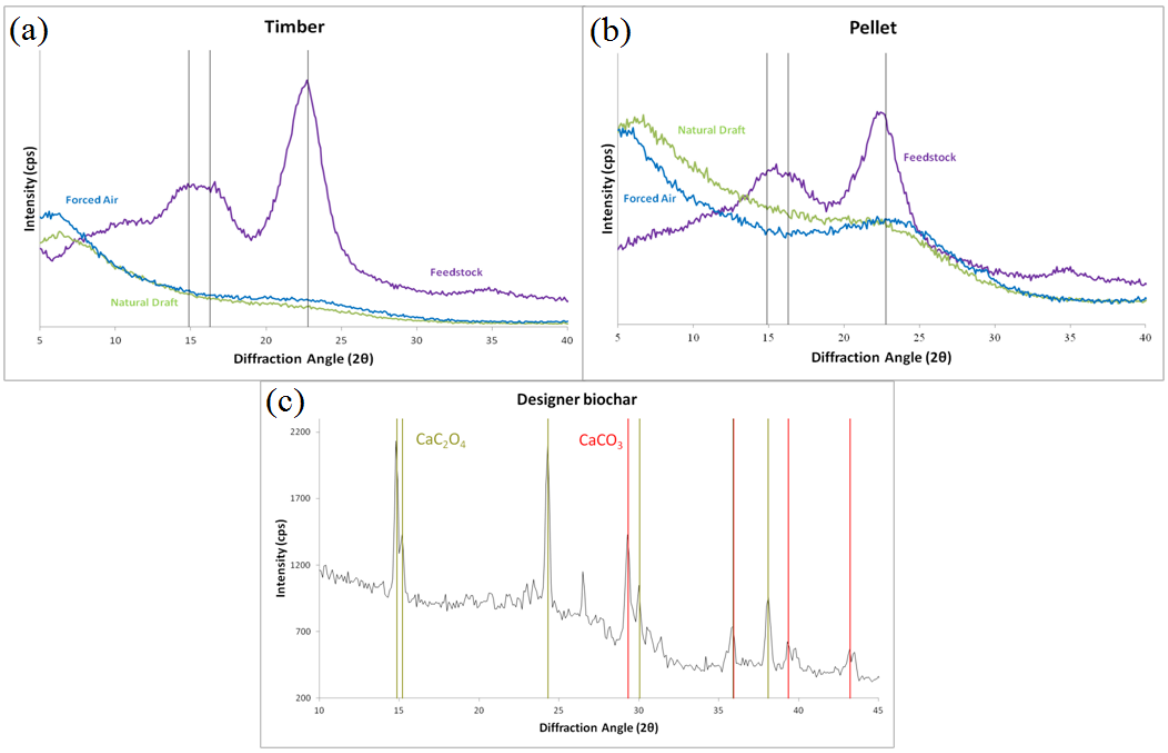

Figure 18: Powder diffraction patterns showing (a) complete cellulosic degredation in timber biochars, (b) partial degredation in pellet biochars and (c) exclusive whewellite [$Ca(C_2O_4)\cdot H_2O$] and calcite [$CaCO_3$] content in designer biochar.

4.4 FTIR

Pine feedstocks exhibit absorption bands centered on 1055 cm^{-1} and 2925 cm^{-1} corresponding to C-OH stretching vibration in secondary alcohol groups and aliphatic C-H stretching vibration of cellulose, respectively [16] [17]. In addition, the broad peak in feedstock spectra between 3200-3500 cm^{-1} can be assigned to the multitude of O-H stretching frequencies in cellulose I [17]. The disappearance of these bands in biochar spectra correlates to a loss of cellulosic content; the sharp presence of the 2850-2925 cm^{-1} doublet in pellet forced air biochar indicates a partial degradation of cellulose I consistent with XRD. Both pellet biochars show a doublet at 2330-2360 cm^{-1} corresponding to a concentration of CO2 greater than atmospheric, most likely adsorbed within micropores [18]. Little evidence of aromatic bonds was present in any biochar spectra, as seen by the weak response for aromatic C-H and aromatic C=C at

875 cm^{-1} and 1585 cm^{-1}, respectively. Designer biochar closely followed expectations: a weak and sharp peak at 875 cm^{-1} for the minimal presence of aromatic C-H, a broad band centered on 1430 cm^{-1} for asymmetric C-O stretching in carbonates and a strong band centered on 1615 cm^{-1} for many frequencies of H_2O bending vibrations [17] [19] [20] (Figure 19).

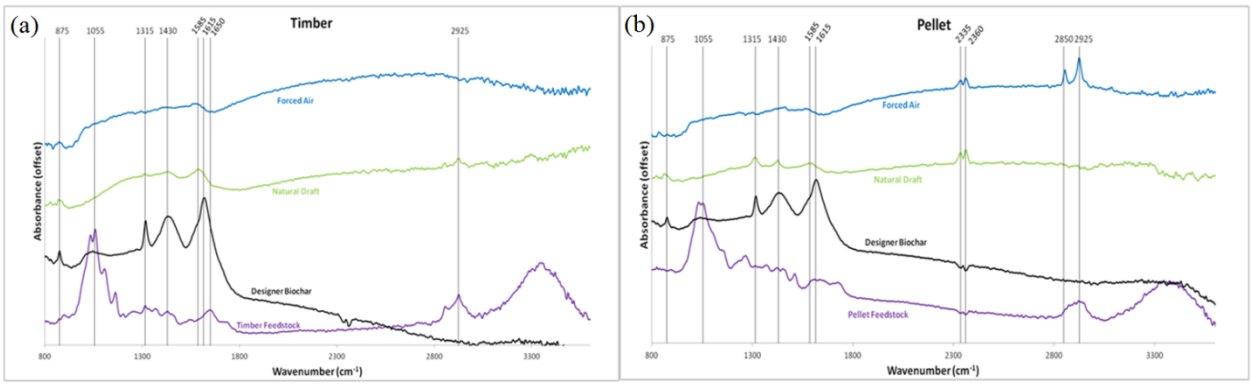

Figure 19: Infrared spectra of (a) timber and (b) pellet biochars and feedstocks. Designer biochar is superimposed on both for direct comparison.

4.5 Carbon / Nitrogen Ratio

The carbon and nitrogen concentrations were determined through dry combustion (Table IV). The C/N ratio was calculated by dividing the total carbon present by the total nitrogen (Figure 20).

Table IV: Concentration of carbon and nitrogen in biochar

Feedstock	Process	Carbon Content	Nitrogen Content
Pellet	Feedstock	47.99	0.046
	Natural	39.04	0.196
	Forced	59.08	0.14
Timber	Feedstock	44.76	0.089
	Natural	52.4	0.104
	Forced	52.03	0.184
Designer	Anerobic	50.28	0.876

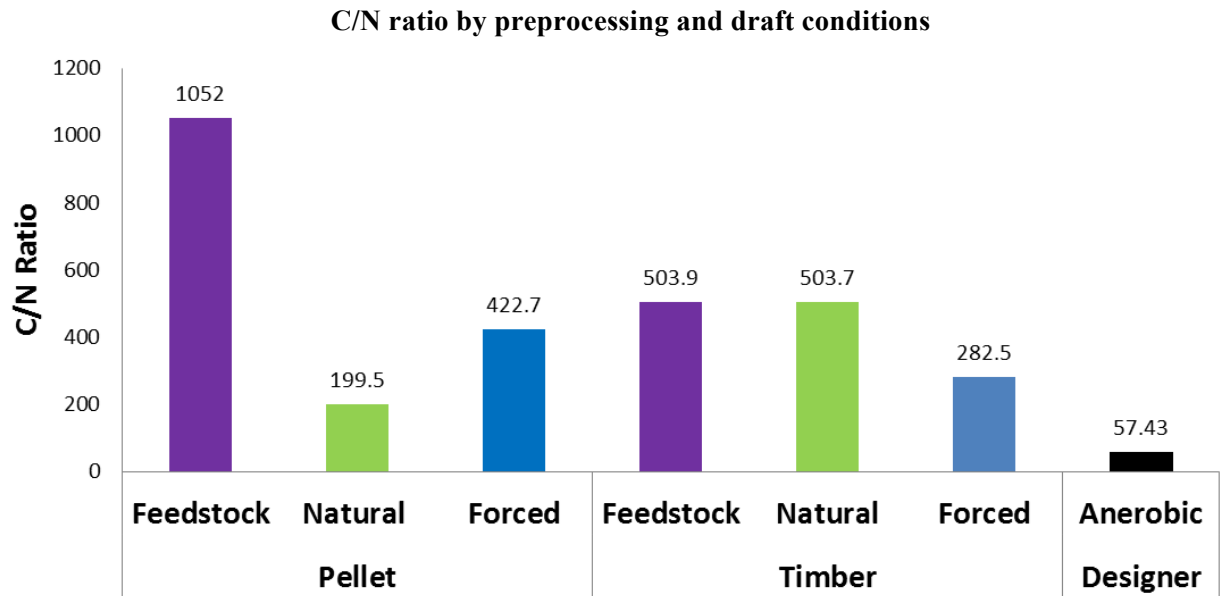

Figure 20: The designer biochar presents a desirable, low C/N ratio, especially compared to the large ratio of the feedstock.

5 Discussion

The high C/N ratio can be attributed to the high pyrolysis temperature where nitrous oxide was able to form and be removed from the reaction. The thermal degradation of both feedstocks into biochar produced lower C/N ratios. No conclusive trends appeared for forced and draft air conditions. Pore morphology appears entirely dependent on preprocessing and minimally influenced by draft conditions. Microchannels in timber biochars could greatly increase active surface area and thus nutrient adsorption.

The loss of cellulose I is evident in both timber and pellet biochars by the deflation of these peaks, albeit only partially in the pellet condition. Hydrated minerals have characteristic changes in crystal structure from their precursors (e.g. hydrating whewellite corrugates the lattice of calcium oxalate via hydrogen bonding) [21]. The mineral hydration of designer biochar propels the negative surface charge, evident by the markedly higher CEC. FTIR spectra of pine biochars show complete degradation of organic content, but do not indicate significant formation of aromatic carbon, meaning the presence of turbostatic graphite cannot be confirmed. Presence and relative intensities of FTIR absorbance peaks of designer biochar are consistent with the high hydrogenated mineral content and minimal presence of aromatic carbon or cellulosic content.

The difference in CECs between biochars can be attributed to several different reasons. Previous research indicates that maximum pyrolysis temperature influences CEC; higher pyrolysis temperatures produce biochars with greater CECs [22]. This trend was observed within the pellet feedstock. The forced air attachment produced a higher pyrolysis temperature than the natural draft and increased CEC. A hypothesis for no statistical difference able to be discerned between the CECs of the timber biochars is their residence time in the reactor. Fast pyrolysis has been shown to produce CECs two times greater than slow pyrolysis or gasification [23]. Since the timber biochars had similar residence times, their CEC values would also be similar. This is in contrast with the pellet biochars that had a much greater difference in residence times as well as a larger difference in CEC. Starting feedstock is a large contributor in biochar CEC and can explain the large discrepancy in CEC between the various feedstocks [22]. This can also account for the the designer biochar having a CEC almost two times greater than any biochar in this study produced from a decentralized reactor.

6 Conclusions

1. A decentralized reactor can achieve pyrolysis temperatures above 900°C, placing the reaction in the gasification region.
2. Forced air method increases process temperature while decreasing burn duration, effectively increasing CEC values.
3. Timber biochars demonstrate complete cellulose I degradation, while pellet biochars show partial or incomplete degradation.
4. Surface morphology is negligibly affected by draft conditions, but heavily influenced by pre-processing.

Bibliography

[1] P. A. F. E. S. a. T. B. R. H. McLaughlin, "All Biochars are Not Created Equal and How to Tell Them Apart," International Biochar Initiative, 2009.

[2] S. G. E. B. H. Moses Hensley Dukua, "Biochar Production Potential in Ghana—A Review," *Renewable and Sustainable Energy Reviews,* vol. 15, pp. 3539-3551, 2011.

[3] C. K. H. C. M. G.-P. J. Y. David Granatstein, "Use of Biochar from the Pyrolysis of Waste Organic Material as a Soil Amendment," Center for Sustaining Agricultue and Natural Resources, Pullman, Washington, 2009.

[4] "All Biochars are not created equal and how to tell them apart".

[5] S. J. A. B. M. v. d. V. I. D. F. Verheijen, "Biochar Application to Soils: A Critical Scientific Review of Effects on Soil Properties, Processes and Functions," JRC Scientific and Technical Reports, Ispra, Italy, 2010.

[6] K. M. C.-A. Y. L. P. M. C. H. C. J. H. L. v. Z. S. K. A. C. B. P. S. J. L. N. F. J. S. a. J. E. A. S. D. Joseph, "An Investigation into the rections of biocahr in soil," *Australian Journal of Soil Research,* vol. 48, pp. 501-514, 2010.

[7] F. Z. A. D. R. H. F. O. V. L. M. S. M. H. G. a. G. S. Stefanie Kloss, "Characterization of Slow Pyrolysis Biochars: Effects of Feedstocks and Pyrolysis Temperature on Biochar Properties," American Society of Agronomy, Crop Science Society of America, and Soil Science Society of America, Madison, WI, 2011.

[8] T. B. R. a. P. W. W. Paul S. Anderson, "Micro-Gasification: What it is and why it works," *Boiling Point,* vol. 52, pp. 36-37, 2007.

[9] P. F. D. D. D. R. H. B. W. c. D. L. K. a. A. L. a. P. F. a. D. D. D. R. H. B. W. D. L. K. David A. Laird, "Impact of biochar amendments on the quality of a typical Midwestern agricultural soil," *Geoderma,* no. 158, pp. 443-449, 2010.

[10] P. P. Hugh McLaughlin, "1G Toucan TLUD for Biochar Production," Alterna Biocarbon Inc., 2010.

[11] P. P. Hugh McLaughlin, "How to make high and low adsorption biochars for small research studies,"

Alterna Biocarbon Inc..

[12] "Eagle Valley Wood Fuel Pellets, Our Product," Eagle Valley, 2010. [Online]. Available: http://www.eaglevalleyfuelpellets.com/product.php. [Accessed 1 June 2012].

[13] "Sierra Pacific Industries Lumber Products," Sierra Pacific Industries, [Online]. Available: http://www.spi-ind.com/html/products_lumber.cfm. [Accessed 1 June 2012].

[14] C. M. A. M. R. C. G. P. L. R. Valerio Causin, "Forensic differentiation of paper by X-ray diffraction and infrared spectroscopy," *Forensic Science International,* vol. 197, pp. 70-74, 2010.

[15] A. V. M. K. P. C. F. R. Michael Lejeune, "Structural characterization of nanopatterned surfaces," *Surface Science,* vol. 583, pp. L142-146, 2005.

[16] C. M. A. M. R. C. G. P. L. R. Valerio Causin, "Forensic differentiation of paper by X-ray diffraction and infrared spectroscopy," *Forensic Science International,* vol. 197, pp. 70-74, 2010.

[17] S. C. L. S. N. K. C. S. P. R. E.K. Girija, "Crystallization and microhardness of calcium oxalate monohydrate," *Materials Chemistry and Physics,* vol. 52, pp. 253-257, 1988.

[18] M. K. A. K. M. S. T. H. T. Echigo, "Re-investigation of the crystal structure of whewellite and the dehyrdation mechanism of caoxite," *Mineralogical Magazine,* vol. 69, no. 1, pp. 77-88, 2005.

[19] A. V. M. K. P. C. F. R. Michael Lejeune, "Structural characterization of nanopatterned surfaces," *Surface Science,* vol. 583, pp. L142-146, 2005.

[20] F. Z. A. D. R. H. F. O. V. L. M. S. M. H. G. G. S. Stefanie Kloss, "Characterization of Slow Pyrolysis Biochars: Effects of Feedstocks," *Journal of Environmental Quality,* p. 70, 2009.

[21] J. B. P. I. R. Z. D. L. d. G. F. a. D. D. G. Matrajt, "FTIR and Raman analyses of the Tagish Lake meteorite:," *Astronomy and Astrophysics,* vol. 416, pp. 983-990, 2004.

[22] J. Lehmann, "Bio-energy in the black," *The Ecological Society of America,* vol. 5, no. 7, pp. 381-387, 2007.

[23] M. K. B. R. E. S. P. A. C. B. I. C. T. G. R. C. B. James W. Lee, "Characterization of Biochars Produced from Cornstovers for Soil Amendment," *Environmental Science Technology,* vol. 44, pp. 7970-7974, 2010.

[24] P. F. D. D. D. R. H. B. W. c. D. L. K. a. A. L. a. P. F. a. D. D. D. R. H. B. W. D. L. K. David A.

Laird, "Impact of biochar amendments on the quality of a typical Midwestern agricultural soil," *Geoderma,* no. 158, pp. 443-449, 2010.